

## Modeling Thermophoresis Phenomena in Non-Premixed Counterflow Combustion of Particles

Gholamreza Shahriari Moghadam<sup>a</sup>, Navid Malekian<sup>\*a</sup>, Hesam Moghadasi<sup>a</sup>, Mehdi Bidabadi<sup>a</sup>

<sup>a</sup> School of Mechanical Engineering, Department of Energy Conversion, Iran University of Science and Technology (IUST), Narmak, 16846-13114, Tehran, Iran

\*Email address(Corresponding author): navid.malekian@yahoo.com

### Abstract

In this paper, an analytical model is presented to investigate flame structure that contains uniformly distributed volatile fuel particles in an oxidizing gas mixture. A non-premixed counterflow combustion is considered assuming a thin region of reaction where lycopodium particles are assumed as the solid fuel. Also, effective forces including thermophoretic, vaporization process and particles radius variations have been studied in this configuration. As the thermophoresis effect severely increases by approaching the flame front, it reaches a specific value that balances the gravity, drag and buoyancy forces applied on the particle. One dimensional flame propagation in organic cloud of fuel particles is analyzed in which flame structure is divided into pre-heat, vaporization, post-vaporization and post-flame zones. It is assumed that particles as fuel and air as oxidizer move toward stagnation plane from two nozzles in the counterflow configuration. Particles initially vaporize in order to release a specific chemical gas which then enters the oxidation reaction process. For this purpose, conservation equations with specific boundary conditions are solved in each zone. The results show that both burning velocity and flame temperature increase with a rise in volume fraction and a reduction in particles diameter.

**Keywords:** Non-Premixed Combustion, Counterflow, Vaporization, Thermophoretic, Particle Volume Fraction.

### 1. Introduction

In the last decades, researches and investigations on different characteristics of combustible particles are common in the scientific communities and so many research works are devoted to the study of the fundamental properties of these particles [1-3].

Combustion of heterogeneous mixtures, including combustible and oxidizer particles is used in many engineering and safety fields. The combustion mechanisms of two-phase mixtures that are involved with the combustion research of organic particles in configurations such as counterflow, are not fully understood so far [4-6].

Broumand and Bidabadi [7] studied the fundamental aspects of premixed flame propagation in micro-iron dust particles, a mathematical model of a one-dimensional dust flame was developed, with the particle combustion time modeled as a function of

particle diameter. Mostafavi et al. [8] performed experimental research and thermo-gravimetric analysis for lycopodium dust particles. Proust [9] presented a few fundamental aspects of flame initiation and propagation in dust clouds. This paper, contributes to a better understanding of dust explosions, including the incidence of thermal radiation and turbulence. In another study, Proust [10] measured laminar burning speeds and optimum flame temperatures for several combustible dust-air. Han et al. [11] experimentally investigated the flame propagation system through lycopodium dust cloud in a vertical duct based on dust particles behavior. Daou [12] presented the characteristics of strained premixed flames. In this study, he thoroughly studied the effect of heat loss, preferential diffusion and reversibility of reaction. Soltaninejad et al. [13] investigated the effect of Micro-organic dust combustion considering particles thermal resistance. Bidabadi et al. [14] presented of recirculation influence on the combustion of micro organic dust particles. Bidabadi and Rahbari [15] investigated the effect of the temperature difference between the gas and the particles on propagation of premixed flames in a combustible mixture containing uniformly distributed volatile fuel particles. In another study, Rockwell and Rangwala [16] analyzed a premixed dust-air flame, under conditions where a homogenous gas-phase reaction front can exist. Bidabadi et al. [17] studied mathematical modeling of a non-premixed organic dust flame in a counterflow configuration. Variation of flame position based on Lewis numbers of fuel and oxidizer was evaluated. Also, mass fraction and temperature profiles of oxidizer and fuel were presented.

Several forces are applied on a particle. Thermophoretic force is due to the particle movement in the direction opposite to temperature gradient. In the transport of soot particles, this force is significant. In non-premixed combustion [18-21], it was observed that the soot particle was warded off from the flame zone because of thermophoresis effect which promoted soot deposition and caused the larger soot accumulation formation. The thermophoretic deposition of particles on the cylindrical tube was studied by Walsh et al. [22]. Moreover, Bidabadi et al. [23] studied the role of thermophoresis on the particle

accumulation and velocity distribution while the flame was propagating through micro-sized iron particles. The current paper presents an analytical investigation of flame propagation (non-premixed counterflow combustion) in lycopodium particles with thermophoresis phenomena. Lagrangian equation is used to discrete the particles by considering gravity, buoyancy, drag and thermophoretic forces. The temperature profile in the thermophoretic force equation is derived from solving the energy conservation equation in the flame structure consisting of four zones. Consequently, the temperature and mass fractions distributions and burning velocity of lycopodium particles are analytically obtained. The results show that both burning velocity and flame temperature increase with a rise in volume fraction and a reduction in particles diameter.

## 2. Governing equations

In this research, the counterflow configuration is considered so that organic particles come from  $-\infty$  and move toward the stagnation plane and the oxidizer path is from  $+\infty$ . At first, fuel particles vaporize to produce a gaseous fuel with a specific chemical structure. Surface reactions will be ignored as well. Next, gaseous fuel will enter to the combustion process with oxidizer. The position of flame formation depends on initial conditions which can occur in the up or down side of stagnation plane. Changing the initial conditions will lead to a change in this position. The structure of diffusion counterflow combustion of organic particles is shown in Figure 1 in a model with thin reaction zone. Fuel particles in a zone which is called vaporization zone, vaporize and a gaseous fuel will be formed. The gaseous fuel reacts with oxidizer flow in an asymptotic zone which is called flame front. The flame front position can be formed on the sides of the stagnation plane which depends on the initial conditions of the problem. As can be seen in this figure, the flame position is located at the up side of the stagnation plane which also can be imagined in the down side as well.

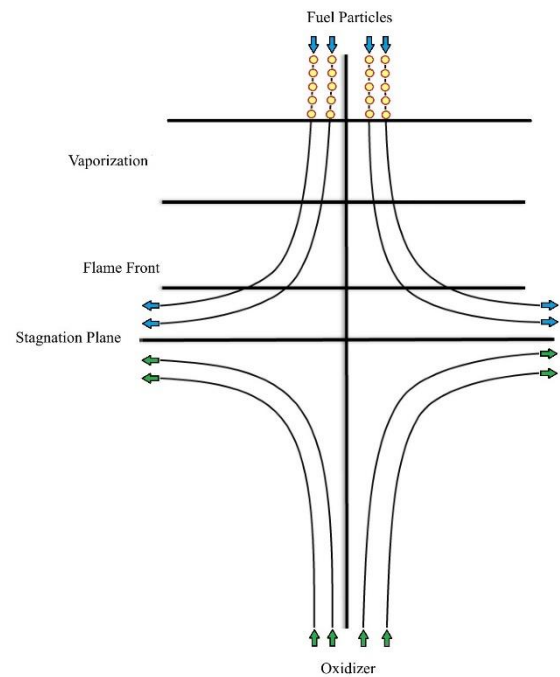


Figure. 1 Structure of diffusion counterflow combustion

In the organic particles combustion, the vaporization rate defined as produced gaseous fuel mass per unit volume and time, is a controller parameter of combustion process. In this research, vaporization rate is considered as:

$$\omega_v = \frac{Y_s}{\tau_v} H(T - T_v) \quad (1)$$

In which  $Y_s$  is mass fraction of solid fuel defined as below:

$$Y_s = \frac{m_p}{m_u} = \left(\frac{r_p}{r_u}\right)^3 \frac{n_p}{n_u} \quad (2)$$

Also,  $\tau_v$  is characteristic time of vaporization,  $T$  and  $T_v$  are fuel and vaporization temperatures and  $H$  is Heaviside function.

Another factor which controls the combustion process is Lewis number. The Lewis number is defined as ratio of heat diffusion to mass diffusion, thus:

$$Le = \frac{\lambda}{\rho C D} \quad (3)$$

Where  $\lambda$ ,  $\rho$ ,  $C$  and  $D$  are conductivity, density, specific heat and mass diffusive coefficient, respectively.

Chemical kinetic is assumed as a general one-stage reaction. Furthermore, Velocity field is considered as  $(u, v) = (-aX, aY)$  where  $u$  and  $v$  are velocities in  $X$  and  $Y$  directions.

### 2.1 Particles Volume Fraction

As is shown in Figure 2, a large enough control volume in flame front which contains adequate number of particles is considered in order to calculate the number density of particles or particles volume fraction. Particles crossing the control volume are assumed to move in an approximately vertical direction. The change in the number density of particles passing through this control volume can be obtained by balancing mass fluxes of particles that

enter and leave the noted control volume. For a continuum medium, density can be defined as the ratio of mass to volume at any point, but in a gas-solid flow, the volume fraction of each phase is related to the bulk or apparent density. The particles volume fraction is defined as:

$$\psi = \frac{V_P}{V} = \frac{m_u n_u Y_s}{\rho_P} \quad (4)$$

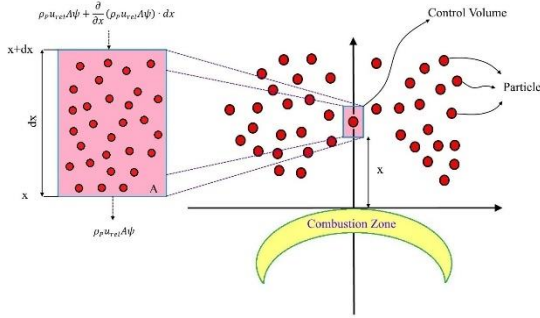


Figure 2 Variations of particles volume fraction in a selected control volume

Steady state conservation equation of mass is expressed as:

$$\frac{\partial(\rho_P u_{rel} \psi)}{\partial X} = \omega_v \quad (5)$$

In which  $u_{rel}$  is particles velocity relative to burning velocity at the leading edge of combustion zone.

$$u_{rel} = u_P - S_L \quad (6)$$

Combining Eqs. (2) and (4), particle radius can be written as:

$$r_P = \left( \frac{m_u n_u Y_s^2}{\psi \rho_P} \right)^{\frac{1}{3}} r_u \quad (7)$$

### 2.2 Mass conservation of solid fuel

If the solid particles diffusion is negligible and with this assumption which solid particles don't have any reactions together, the mass conservation of solid fuel particles is written as:

$$-aX \frac{dY_s}{dX} = -\omega_v \quad (8)$$

Where  $Y_s$  is mass fraction of solid particles and  $\omega_v$  is the vaporization rate which has been defined in Eq. (1), previously.

### 2.3 Mass conservation of gaseous fuel

$$-aX \frac{dY_F}{dX} = D_F \frac{d^2 Y_F}{dX^2} - \frac{\omega_F}{\rho} + \omega_v \quad (9)$$

Where  $D_F$  and  $Y_F$  are mass diffusivity of fuel and mass fraction of gaseous fuel, respectively.  $\omega_F$  is the rate of chemical reaction which follows the Arrhenius rule and is in the first order relative to fuel and oxidizer. It is define as:

$$\omega_F = B \rho^2 v_F v_O \bar{Y}_F \bar{Y}_O \exp\left(-\frac{E}{RT}\right) \quad (10)$$

### 2.4 Mass conservation of oxidizer

$$-aX \frac{dY_O}{dX} = D_O \frac{d^2 Y_O}{dX^2} - \vartheta \frac{\omega_F}{\rho} \quad (11)$$

In the above equation,  $D_O$ ,  $Y_O$  and  $\vartheta$  are oxidizer mass diffusivity, oxidizer mass fraction and stoichiometric mass ratio of oxygen to fuel, respectively.

### 2.5 Energy conservation of mixture

$$-aX \frac{dT}{dX} = D_T \frac{d^2 T}{dX^2} + \omega_F \frac{Q}{\rho C} - \omega_v \frac{Q_v}{C} \quad (12)$$

Where  $Q$  is the heat released per unit of consumed fuel mass,  $Q_v$  is the latent vaporization heat of particles and  $Q_{rad}$  is radiation heat transfer. Also,  $D_T$  is thermal diffusivity and  $C$  is specific heat of mixture which is obtained from combination of gaseous phase specific heat  $C_a$  and solid particles specific heat  $C_p$  as below:

$$C = C_a + \frac{4}{3} \pi r_P^3 n_P \frac{\rho_P}{\rho} C_P \quad (13)$$

Where  $\rho_P$  is the solid particle density and  $n_P$  shows the number of particles per unit of volume. Thus:

$$\rho = \rho_a + \frac{4}{3} \pi r_P^3 n_P \rho_P \quad (14)$$

### 2.6 Effective forces

In the Lagrangian approach, particle Brownian motion is neglected and individual particle trajectories (position and velocity as a function of time) are determined by integrating the following ordinary differential equation

$$\sum F = \frac{d(m_P u_P)}{dt} \quad (15)$$

Various forces affect particle motion are defined as below:

- **Gravity force**

A particle can be subjected to the gravity force that is proportional to its mass. For a spherical particle, the gravity force can be written as:

$$F_g = \frac{4}{3} \pi r_P^3 \rho_P g \quad (16)$$

Where  $r_P$ ,  $\rho_P$  and  $g$  are particle radius, particle density and gravity acceleration, respectively.

- **Buoyancy force**

Since the particle is assumed to be completely submerged in air, buoyancy force is exerted on the particle which is defined as an upward force caused by fluid pressure that opposes the gravity force. Buoyancy force can be written as:

$$F_B = \frac{4}{3} \pi r_P^3 \rho_g g \quad (17)$$

Where  $\rho_g$  is the surrounding gas density.

- **Drag force**

A particle moving at a different velocity than that of the surrounding gas will experience fluid (gas) resistance or an opposing drag force by the fluid. At low Reynolds numbers, the drag force on a rigid sphere of radius  $r_P$  is determined by the Stokesian approximation as:

$$F_D = -6\pi\mu r_P u_{rel} \quad (18)$$

In which  $\mu$  is the gas viscosity and  $u_{rel}$  indicates relative velocity.

- **Thermophoretic force**

Experimental data show that thermophoretic is strongly dependent on the Knudsen number defined as:

$$Kn = \frac{\lambda}{r_p} \quad (19)$$

Considering small Knudsen numbers, the Talbot's equation for thermal force near a continuum limit is:

$$F_{Th} = -12\pi\mu^2 r_p k_T \frac{\nabla T}{\rho_g T_\infty} \quad (20)$$

In which

$$k_T = \frac{2C_{P,Th} \left( \frac{k_g}{k_p} + C_{C,Th} Kn \right)}{(1 + 3C_m Kn) \left( 1 + 2 \frac{k_g}{k_p} + 2C_{C,Th} Kn \right)} \quad (21)$$

Where  $\nabla T$ ,  $T_\infty$ ,  $k_p$ ,  $k_g$ ,  $C_{C,Th}$ ,  $C_{P,Th}$  and  $C_m$  are temperature gradient, surrounding gas temperature, gas kinematics viscosity, lycopodium particle thermal conductivity, gas thermal conductivity, thermal creep coefficient, temperature jump coefficient and velocity jump coefficient, respectively.

### 2.7 Dimensionless form of the governing equations

For dimensionless form of the equations, some variables are defined as below.

$$x = \frac{X}{\sqrt{\frac{\lambda}{\rho C a}}} \quad (22)$$

$$y_s = \frac{Y_s}{Y_{F-\infty}}$$

$$y_F = \frac{Y_F}{Y_{F-\infty}}$$

$$y_o = \frac{Y_o}{Y_{F-\infty}}$$

$$\theta = \frac{C(T - T_\infty)}{Q Y_{F-\infty}}$$

$Y_{F-\infty}$  is the mass fraction of fuel at the position  $-\infty$  where the fuel is coming from the fuel nozzle. Here,  $T_\infty$  represents the temperature in the outlets of nozzles. By substituting dimensionless parameters into the conservation equations, dimensionless conservation equations will be achieved.

Dimensionless equation of solid fuel mass conservation is given by:

$$x \frac{dy_s}{dx} = \frac{y_s}{\alpha \tau_v} H(\theta - \theta_v) \quad (23)$$

Dimensionless equation of gaseous fuel mass conservation is given by:

$$\frac{1}{Le_F} \frac{d^2 y_F}{dx^2} + x \frac{dy_F}{dx} + \frac{y_s}{\alpha \tau_v} H(\theta - \theta_v) = D_c y_F y_o \exp\left(-\frac{T_a}{T}\right) \quad (24)$$

$T_a$  shows dimensionless activation energy which  $T_a = \frac{E}{R}$ . Also,  $D_c$  is defined as:

$$D_c = \frac{\rho B \vartheta_o Y_{F-\infty}}{W_F a} \quad (25)$$

In which  $\vartheta_o$  is the number of stoichiometric oxygen moles reacting with one mole of fuel and  $W_F$  is the molecular weight of the fuel.

Dimensionless equation of oxidizer mass conservation is given by:

$$x \frac{dy_o}{dx} + \frac{1}{Le_o} \frac{d^2 y_o}{dx^2} = D_c y_F y_o \exp\left(-\frac{T_a}{T}\right) \quad (26)$$

Dimensionless equation of energy conservation is given by:

$$\frac{d^2 \theta}{dx^2} + x \frac{d\theta}{dx} - \frac{q y_s}{\alpha \tau_v} H(\theta - \theta_v) = -D_c y_F y_o \exp\left(-\frac{T_a}{T}\right) \quad (27)$$

In which  $q = \frac{Q_v}{Q}$ .

### 2.8 Boundary Conditions

To solve equations, it is necessary to apply the boundary conditions. For instance, at flame position, one can write:

$$\frac{dy_F}{dx} \Big|_{x_f^-} = \frac{Le_F}{Le_o} \frac{dy_o}{dx} \Big|_{x_f^-}$$

$$\frac{dy_F}{dx} \Big|_{x_f^+} = -Le_F \frac{d\theta}{dx} \Big|_{x_f^+}$$

$$\frac{dy_o}{dx} \Big|_{x_f^+} = -Le_o \frac{d\theta}{dx} \Big|_{x_f^+}$$

$$y_F \Big|_{x_f^+} = y_o \Big|_{x_f^+} = \theta \Big|_{x_f^+} = 0 \quad (28)$$

### 3. Solving Equations

By solving conservation equations and applying boundary conditions, gaseous fuel mass fraction, oxidizer mass fraction and temperature distributions are achieved in each zone.

Gaseous fuel mass fraction distribution in pre-flame zone is given by:

$$y_F = y_{Fv} \frac{\operatorname{erf}\left(x \sqrt{\frac{Le_F}{2}}\right) + 1}{\operatorname{erf}\left(x_v \sqrt{\frac{Le_F}{2}}\right) + 1}$$

$$y_F = y_{Fv} \frac{\operatorname{erf}\left(x \sqrt{\frac{Le_F}{2}}\right) - \operatorname{erf}\left(x_f \sqrt{\frac{Le_F}{2}}\right)}{\operatorname{erf}\left(x_v \sqrt{\frac{Le_F}{2}}\right) - \operatorname{erf}\left(x_f \sqrt{\frac{Le_F}{2}}\right)} \quad (29)$$

Where  $\operatorname{erf}(x)$  is the error function defining as:

$$\operatorname{erf}(x) = \frac{2}{\sqrt{\pi}} \int_0^x e^{-t^2} dt \quad (30)$$

Gaseous fuel mass fraction distribution in post-flame zone is given by:

$$y_F = 0 \quad (31)$$

Oxidizer mass fraction distribution in pre-flame zone is given by:

$$y_o = 0 \quad (32)$$

Oxidizer mass fraction distribution in post-flame zone is given by:

$$y_o = \alpha \frac{\operatorname{erf}\left(x \sqrt{\frac{Le_o}{2}}\right) - \operatorname{erf}\left(x_f \sqrt{\frac{Le_o}{2}}\right)}{1 - \operatorname{erf}\left(x_f \sqrt{\frac{Le_o}{2}}\right)} \quad (33)$$

Temperature distribution in pre-flame zone is given by:

$$\theta = \theta_v \frac{\operatorname{erf}\left(\frac{x}{\sqrt{2}}\right) + 1}{\operatorname{erf}\left(\frac{x_v}{\sqrt{2}}\right) + 1}$$

$$\theta = \frac{\theta_v - \theta_f}{\operatorname{erf}\left(\frac{x_v}{\sqrt{2}}\right) - \operatorname{erf}\left(\frac{x_f}{\sqrt{2}}\right)} \operatorname{erf}\left(\frac{x}{\sqrt{2}}\right) + \frac{\theta_f \operatorname{erf}\left(\frac{x_v}{\sqrt{2}}\right) - \theta_v \operatorname{erf}\left(\frac{x_f}{\sqrt{2}}\right)}{\operatorname{erf}\left(\frac{x_v}{\sqrt{2}}\right) - \operatorname{erf}\left(\frac{x_f}{\sqrt{2}}\right)} \quad (34)$$

Also, temperature distribution in post-flame zone is given by:

$$\theta = \theta_f \frac{\operatorname{erf}\left(\frac{x}{\sqrt{2}}\right) - 1}{\operatorname{erf}\left(\frac{x_f}{\sqrt{2}}\right) - 1} \quad (35)$$

#### 4. Particle Dynamics

The pre-heat zone is divided into two areas delineated by the ranges of  $-\infty < x < x_t$  and  $x_t < x < x_v$ . In fact, at a distance, thermophoretic force can be considered ignorable. Thus, at this certain position, particle moves with a constant velocity. This position can be obtained using [11, 24]:

$$x_t = \left(\frac{\rho_p}{m_u n_u}\right)^{0.1} \left(\frac{\rho_g S_L C}{k_g} D\right)^{0.2} x_v \quad (36)$$

By approaching the flame front, thermophoretic force rises. Hence, particle velocity reaches to zero at a certain position in which it can't move anymore. This position is called free particle distance and is achieved by solving Eq. (15) as:

$$x^* = \sqrt{-\ln\left(\frac{\sqrt{\pi} \rho_g T_m r_p^2 (\rho_p - \rho_g) (k_p + 2k_g) \left[\operatorname{erf}\left(\sqrt{\frac{D a_{str}}{2}} x_f\right) + 1\right]}{36 \mu^2 C_{p,Th} k_g (T_f - T_u)}\right)} \quad (37)$$

- Zone  $-\infty < x < x_t$

Thermophoretic force can be considered negligible in this zone. Therefore, drag, buoyancy and gravity forces are balanced as:

$$6\pi\mu r_p u_t + \frac{4}{3}\pi r_p^3 \rho_g g = \frac{4}{3}\pi r_p^3 \rho_p g \quad (38)$$

In this zone, particle moves with a constant velocity which is derived as:

$$u_t = \frac{2 r_p^2 g}{9 \mu} (\rho_p - \rho_g) \quad (39)$$

Also, particle volume fraction remains constant and is computed by:

$$\bar{\psi} = \frac{m_u n_u}{\rho_p} \quad (40)$$

- Zone  $x_t < x < x_v$

In this zone, thermophoretic force is dominant. Thus, motion equation is stated as:

$$-24\pi\mu^2 r_p C_{p,Th} \frac{k_g}{k_p + 2k_g} \frac{\nabla T}{\rho_g T_m} = m_p u_p \frac{du_p}{dX} \quad (41)$$

Temperature gradient is calculated by deriving temperature equation in the related zone.

$$\nabla T = \frac{2(T_v - T_u) \exp\left(-\frac{x^2}{2}\right)}{\sqrt{\pi} \left[1 + \operatorname{erf}\left(\frac{x_v}{\sqrt{2}}\right)\right]} \quad (42)$$

Substituting Eq. (42) into Eq. (41), integrating and applying boundary condition at  $x = x_v$ , the following equation is acquired.

$$u_p^2 = u_t^2 + 2\beta \left[\operatorname{erf}\left(\frac{x}{\sqrt{2}}\right) - \operatorname{erf}\left(\frac{x_t}{\sqrt{2}}\right)\right] \quad (43)$$

In which

$$\beta = -\frac{24\pi\mu^2 r_p C_{p,Th}}{m_u \rho_g T_m} \frac{k_g}{k_p + 2k_g} (T_v - T_u) \quad (44)$$

In this zone, rate of vaporization is equal to zero, therefore particle conservation equation is written as:

$$\frac{\partial(\psi u_{rel})}{\partial X} = 0 \quad (45)$$

$$\psi u_{rel} = \text{const} \quad (46)$$

$$\psi u_{rel} = \bar{\psi}(u_t - S_L) \quad (47)$$

Thus, particle volume fraction is computed as:

$$\psi = \frac{u_t - S_L}{u_p - S_L} \bar{\psi} \quad (48)$$

- Zone  $x_v < x < x^*$

Using Newton's second law, motion equation can be written as:

$$-24\pi\mu^2 r_p C_{p,Th} \frac{k_g}{k_p + 2k_g} \frac{\nabla T}{\rho_g T_m} = m_p \frac{d(m_p u_p)}{dX} \quad (49)$$

In which  $m_p$  and  $r_p$  are mass and radius of a particle in the vaporization zone, respectively. Eliminating these two terms using Eqs. (2) and (7), considering temperature gradient in the vaporization zone, using Runge-Kutta method and solving nonlinear Eq. (49), particle velocity is computed in this zone.

#### Result and discussion

Organic fuel of lycopodium particles are considered and the value of quantities utilized in conservation equations will be obtained using their properties. It is necessary to note that these particles are of organic type that release combustible gases while receiving heat. In Table 1, lycopodium properties are presented [3, 21, 25].

Table 1 Properties used in the solution

Property	Value
$\rho_p$	1000 $\frac{kg}{m^3}$
$\rho_a$	1.164 $\frac{kg}{m^3}$
$C_p$	5.677688 $\frac{kJ}{kg \cdot K}$
$C_a$	1.00416 $\frac{kJ}{kg \cdot K}$
$Q$	64895.4 $\frac{kJ}{kg}$
$k_p$	$1.46538 \times 10^{-4} \frac{kJ}{m \cdot s \cdot K}$
$k_g$	$0.3468 \times 10^{-4} \frac{kJ}{m \cdot s \cdot K}$
$C_{p,Th}$	1.14
$C_{c,Th}$	2.2
$C_m$	1.146

The released gas from lycopodium is considered to be methane [16, 25]. The combustion reaction is denoted as:

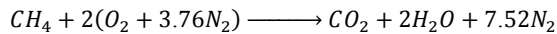


Figure 3 depicts a comparison between temperature profiles of gaseous fuel and oxidizer with respect to flame position for different oxidizer Lewis numbers. As is clear in the figure, the gaseous fuel and oxidizer temperatures are located at the left and right side of the diagram, respectively. The temperatures gradually increase to achieve flame temperature.

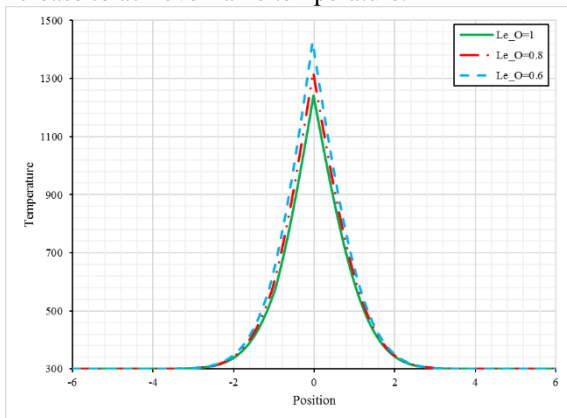


Figure 3 Temperature profiles of fuel and oxidizer for different oxidizer Lewis numbers

Figures 4 and 5 respectively show the comparison between gaseous fuel mass fraction and oxidizer mass fraction versus various gr positions at the mass concentration of 100 gr/m<sup>3</sup> for different fuel and oxidizer Lewis numbers. As can be observed in Figure 4, gaseous fuel mass fraction rises until reaches to a maximum point at the vaporization position and then, slowly decreases until reaches to zero at the flame formation position. As can be seen in Figure 5, by decreasing initial mass fraction of oxidizer, a lower maximum will be obtained and by getting closer to the flame formation position, mass fraction of oxidizer gradually decreases until reaches to the flame position and then, achieves the value of zero.

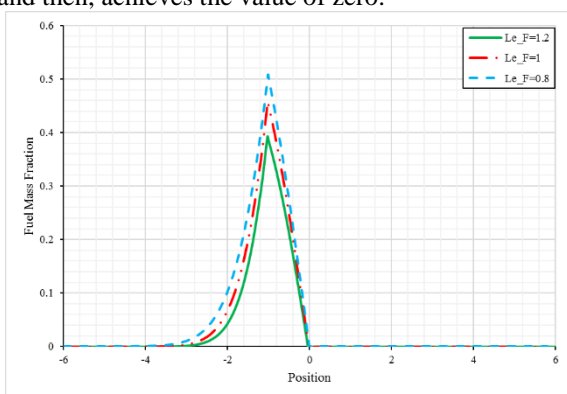


Figure 4 Mass fraction profile of fuel for different Fuel Lewis numbers

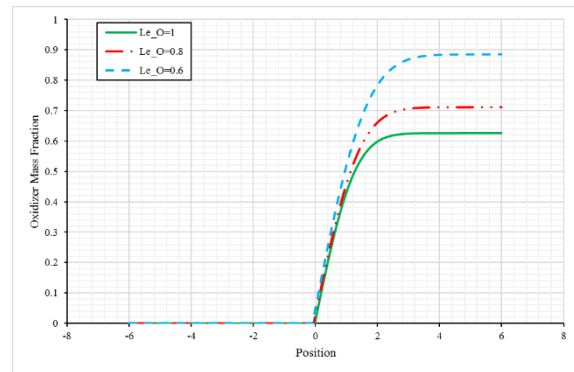


Figure 5 Mass fraction profile of oxidizer for different oxidizer Lewis numbers

Figure 6 shows flame temperature variations with respect to fuel Lewis number for two different mass concentrations of particles. As mentioned previously, Lewis number is defined as the ratio of heat diffusion to the mass diffusion. In this figure, increasing fuel Lewis number is equivalent to reduction in mass fraction, thus this decrease will cause the flame temperature to reduce. Also, increasing mass concentration from 67 gr/m<sup>3</sup> to 83 gr/m<sup>3</sup> will cause a growth in flame temperature. By increasing fuel mass concentration, the amount of available fuel will increase and then, by reacting more fuel, flame temperature increases as well. The vaporization temperature used in this paper was obtained from Proust researches [9, 10]. It should be noted that oxidizer Lewis number is assumed to be unit and the initial equivalence ratio is equal to  $\phi = 1.4$ .

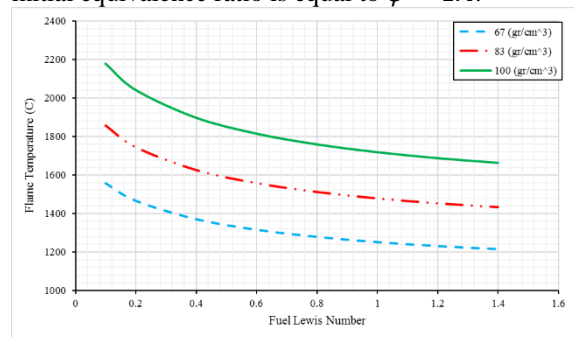


Figure 6 Flame temperature variations with respect to fuel Lewis number for two different mass concentrations of particles

In Figures 7 and 8, burning velocity and flame temperature are demonstrated against particle volume fraction, far from the combustion zone, for different radiuses of particle. As these figures show, by reducing initial particle radius or rising particle volume fraction, the surface-to-volume ratio of all particles increases and the contact surface between oxidizer and particles becomes bigger. Hence, vaporization resistance of solid fuel particles diminishes, leading to an increase in burning velocity and flame temperature.

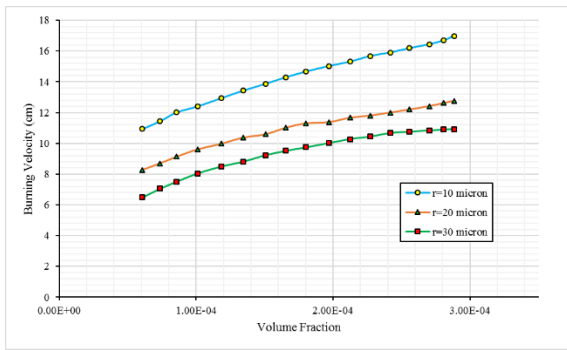


Figure 7 Burning velocity versus particle volume fraction for different radiuses of particle

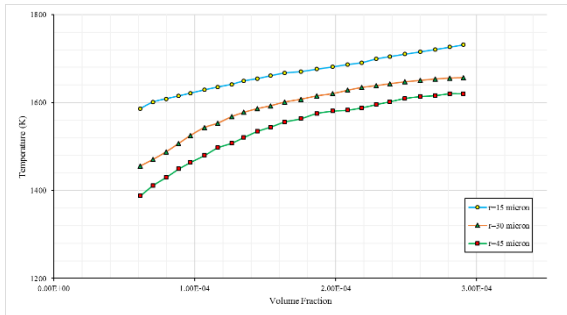


Figure 8 Flame temperature versus particle volume fraction for different radiuses of particle

In Figure 9, variations of free particle distance is plotted in terms of particle radius. By increasing particle radius, effect of gravity force increases. Therefore, thermophoretic force overcomes gravity force in a closer distance to the flame position. That's why free particle distance decreases by making a rise in particle radius.

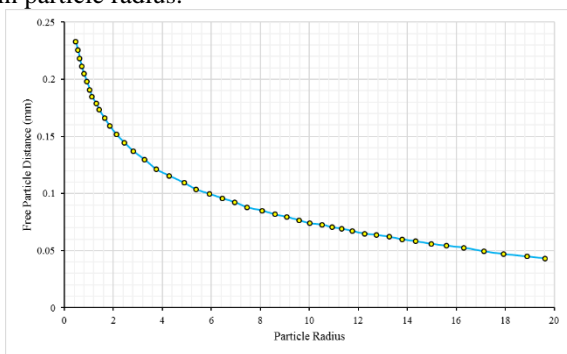


Figure 9 Variations of free particle distance in terms of particle radius

### Conclusion

In this paper, the combustion of organic particles in counterflow configuration was considered taking into account three zones and assuming the asymptotic zones for vaporization and reaction. Assuming particles to vaporize first to produce a specific chemical gas, gaseous fuel mass fraction and oxidizer mass fraction along with the energy equation were written using specific boundary conditions and solved by mathematical methods. By using boundary conditions, the conditions were determined in vaporization and reaction zones which required a simultaneous solution. The above equations were solved using numerical methods for solving nonlinear algebraic equations. The position and temperature of

the flame were evaluated versus variations of fuel and oxidizer Lewis numbers, different equivalence ratios and different mass concentrations of particles. It was found that by increasing Lewis numbers of fuel and oxidizer, flame temperature decreases and increasing Lewis number of oxidizer moves flame position toward the oxidizer nozzle. Also, increasing mass concentration of particles and reducing particles radius lead to a rise in flame temperature.

### Nomenclature

$a$	Strain rate
$C_a$	Heat capacity of gaseous fuel
$C_{C,Th}$	Temperature jump coefficient
$C_m$	Velocity jump coefficient
$C_p$	Heat capacity of solid particle
$C_{P,Th}$	Thermal creep coefficient
$D_F$	Mass diffusivity of gaseous fuel
$D_O$	Mass diffusivity of oxidizer
$D_T$	Thermal conductivity
$H$	Heaviside function
$k_g$	Thermal conductivity of gas
$k_p$	Thermal conductivity of particle
$Kn$	Knudsen number
$Le$	Lewis number

$m$	Molecular weight of mixture
$m_f$	Molecular weight of fuel
$m_O$	Molecular weight of oxidizer
$n_p$	Number of particles per unit volume
$Q$	Heat of reaction
$Q_v$	Latent heat of particles vaporization
$R$	Universal gas constant
$r$	Radius
$T$	Temperature
$T_a$	Activation energy
$T_v$	Vaporization temperature
$x_t$	Defined in Eq. (37)
$x^*$	Particle free distance
$Y_F$	Mass fraction of gaseous fuel
$Y_{F-\infty}$	Mass fraction of fuel at a distance of $-\infty$
$Y_O$	Mass fraction of oxidizer
$Y_s$	Mass fraction of solid fuel

**Greek Letters**

$\alpha$	Initial mass fraction oxidizer
$\theta$	Dimensionless temperature
$\vartheta$	Stoichiometric mass ratio of oxidizer to fuel
$\mu$	Dynamic viscosity
$\rho$	Density
$\rho_p$	Density of solid particle
$\tau_v$	Characteristic time of vaporization
$v_F$	Stoichiometric coefficient of fuel
$v_O$	Stoichiometric coefficient of oxidizer
$v_P$	Stoichiometric coefficient of products
$\psi$	Particle volume fraction
$\omega_F$	Rate of the chemical kinetics
$\omega_v$	Vaporization rate of particles

**References**

- [1] Eckhoff, R.K., 2009. Understanding dust explosions. The role of powder science and technology. *Journal of Loss Prevention in the Process Industries*, 22(1), pp.105-116.
- [2] Chen, J.L., Dobashi, R. and Hirano, T., 1996. Mechanisms of flame propagation through combustible particle clouds. *Journal of Loss Prevention in the Process Industries*, 9(3), pp.225-229.
- [3] Han, O.S., Yashima, M., Matsuda, T., Matsui, H., Miyake, A. and Ogawa, T., 2000. Behavior of flames propagating through lycopodium dust clouds in a vertical duct. *Journal of Loss Prevention in the Process Industries*, 13(6), pp.449-457.
- [4] Malekian, N., Moghadasi, H., Bidabadi, M. and Moghadam, G.S., 2017 Efficiency Analysis in a Furnace Regenerator Using Lycopodium Particles. The 25th Annual International Conference on Mechanical Engineering ISME2017, Tarbiat Modares university, Tehran, Iran.
- [5] Moghadasi, H., Malekian, N., Bidabadi, M. and Moghadam, G.S., 2017 An analytical modeling of particles thermal resistance in pre-mixed organic dust (Lycopodium) combustion. The 25th Annual International Conference on Mechanical Engineering ISME2017, Tarbiat Modares university, Tehran, Iran.
- [6] Afzalabadi, A., Poorfar, A.K., Bidabadi, M., Moghadasi, H., Hochgreb, S., Rahbari, A. and Dubois, C., 2017. Study on hybrid combustion of aerosuspensions of boron-aluminum powders in a quiescent reaction medium. *Journal of Loss Prevention in the Process Industries*, 49, pp.645-651.
- [7] Broumand, Mohsen, and Mehdi Bidabadi. "Modeling combustion of micron-sized iron dust particles during flame propagation in a vertical duct." *Fire Safety Journal* 59 (2013): 88-93.
- [8] Mostafavi, Seyed Alireza, et al. "Pyrolysis and combustion kinetics of lycopodium particles in thermogravimetric analysis." *Journal of Central South University* 22.9 (2015): 3409-3417.
- [9] Proust, Christophe. "A few fundamental aspects about ignition and flame propagation in dust clouds." *Journal of Loss Prevention in the Process Industries* 19.2 (2006): 104-120.
- [10] Proust, Christophe. "Flame propagation and combustion in some dust-air mixtures." *Journal of Loss Prevention in the Process Industries* 19.1 (2006): 89-100.
- [11] O.S. Han, M. Yashima, T. Matsuda, H. Matsui, A. Miyake, T. Ogawa, A study of flame propagation mechanisms in lycopodium dust clouds based on dust particles' behavior, *J. Loss Prev. Process Ind.*, 14, (2001), 153-160.
- [12] J. Daou, strained premixed flames: Effect of heat-loss, preferential diffusion and reversibility of the reaction, *Combust. Theory Model.* 15 (4), (2011), 437-454.
- [13] Soltaninejad, M., Dizaji, F. F., Dizaji, H. B., & Bidabadi, M. (2015). Micro-organic dust combustion considering particles thermal resistance. *Journal of Central South University*, 22(7), 2833-2840.
- [14] Bidabadi, M., Fanaee, A., & Rahbari, A. (2010). Investigation over the recirculation influence on the combustion of micro organic dust particles. *Applied Mathematics and Mechanics*, 31(6), 685-696.
- [15] M. Bidabadi, A. Rahbari, Modeling combustion of lycopodium particles by considering the temperature difference between the gas and the particles, *Combust. Expl. Shock Waves*, 45, (2009), 278-285.
- [16] Rockwell, Scott R., and Ali S. Rangwala. "Modeling of dust air flames." *Fire Safety Journal* 59 (2013): 22-29.
- [17] Bidabadi, M., Ramezanpour, M., Khoeini Poorfar, A., Monteiro, E. and Rouboa, A., 2016. Mathematical modeling of a Non-Premixed organic Dust flame in a Counterflow configuration. *Energy & Fuels*, 30(11), pp.9772-9782.

- [18] Fujita, O., and Ito, K., 2002, "Observation of Soot Agglomeration Process With Aid of Thermophoretic Force in a Microgravity Jet Diffusion Flame," *Exp. Therm. Fluid Sci.*, 26(2-4), pp. 305-311.
- [19] Pushkar, T., James, P. T., Xiaodong, F., and Amy, R., 2003, "Estimation of Particle Volume Fraction, Mass Fraction and Number Density in Thermophoretic Deposition Systems," *Int. J. Heat Mass Transfer*, 46(17), pp. 3201-3209.
- [20] Choi, J. H., Fujita, O., Tsuiki, T., Kim, J., and Chung, S. H., 2008, "Experimental Study on Thermophoretic Deposition of Soot Particles in Laminar Diffusion Flames Along a Solid Wall in Microgravity," *Exp. Therm. Fluid Sci.*, 32(8), pp. 1484-1491.
- [21] Rahbari, A., Wong, K.F., Vakilabadi, M.A., Poorfar, A.K. and Afzalabadi, A., 2017. Theoretical investigation of particle behavior on flame propagation in lycopodium dust cloud. *Journal of Energy Resources Technology*, 139(1), p.012202.
- [22] Walsh, K., Weimer, A. W., and Hrenya, C. M., 2006, "Thermophoretic Deposition of Aerosol Particles in Laminar Tube Flow With Mixed Convection," *J. Aerosol Sci.*, 37(6), pp. 715-734.
- [23] Bidabadi, M., Haghiri, A., and Rahbari, A., 2010, "Mathematical Modeling of Velocity and Number Density Profiles of Particles Across the Flame Propagation Through a Micro-Iron Dust Cloud," *J. Hazard. Mater.*, 176(1-3), pp.146-153.
- [24] Han, O.S., Yashima, M., Matsuda, T., Matsui, H., Miyake, A. and Ogawa, T., 2000. Behavior of flames propagating through lycopodium dust clouds in a vertical duct. *Journal of Loss Prevention in the Process Industries*, 13(6), pp.449-457.
- [25] Seshadri, K. and Trevino, C., 1989. The influence of the Lewis numbers of the reactants on the asymptotic structure of counterflow and stagnant diffusion flames. *Combustion science and technology*, 64(4-6), pp.243-261.